A Reliable Singular-Vector Pre-Coded OFDM-DCSK System over Doubly Selective Fading Channels

Zhaofeng Liu, Hing Cheung So, *Fellow, IEEE*, Lin Zhang, *Senior Member, IEEE*, Xiao Peng Li, and Zhi-Yong Wang

***Abstract*—In this paper, we put forth a novel strategy to boost the reliability of orthogonal frequency division multiplexing differential chaos shift keying (OFDM-DCSK) systems over doubly selective fading channels. Provided the accessibility of channel state information, singular value decomposition is exploited to partition the channel into distinct sub-channels, which is realized by multiplying the right singular vectors by the symbol matrix at the transmitter. Subsequently, the sub-channel associated with the largest singular value is allocated to the reference chaotic sequence, leading to a higher signal-to-noise ratio (SNR) of demodulated symbols and lower bit error rate (BER) at the receiver. Inspired by the water-filling principle, the BER can be further reduced by permuting the symbols in a strategic manner. This approach of channel decomposition integrated with symbol reallocation, referred to as singular-vector pre-coded OFDM-DCSK (SVP-OFDM-DCSK), is able to escalate the SNR over doubly selective channels, ultimately enhancing the system reliability. The BER of the SVP-OFDM-DCSK system is also analyzed. Simulation results demonstrate that the proposed system with and without symbol permutation step achieves lower BERs than existing schemes over doubly selective fading channels.**

***Index Terms*—Differential chaos shift keying; doubly selective fading channel; singular value decomposition; bit error rate; reliability.**

I. Introduction

Wireless communication systems are inherently vulnerable to attacks from malicious users due to their openness to surrounding environments and broadcast characteristics. Chaotic communication serves as a powerful encryption technique to protect them from these attacks, owing to the high-security properties of chaotic sequences, including sensitivity to initial values, good auto-correlation, resistance to interference, pseudo-randomness, and ergodicity [1], [2]. In fact, chaotic communication techniques have been widely employed in data transmission for ultra-wide-band (UWB) [1], [3], power line communication (PLC) [4], and vehicle-to-vehicle (V2V) communication [5]. In particular, chaotic modulation uses chaotic sequences to modulate information bits and can be classified into coherent and non-coherent types. The main difference is that coherent modulation requires regeneration of the chaotic sequence at the receiver, while non-coherent modulation does not, making the latter less complex and more popular [6], [7].

Among various non-coherent chaotic modulation schemes, differential chaos shift keying (DCSK) has attracted considerable attention [6]. In DCSK, a reference chaotic sequence is transmitted, and the subsequent information-bearing chaotic sequence is generated by multiplying binary phase shift keying (BPSK) symbols with the reference chaotic sequence. The use of the reference sequence eliminates the need for the receiver to regenerate the chaotic waveform, thus circumventing chaos synchronization and significantly lowering the complexity. In many communication scenarios, such as UWB, PLC, and V2V, DCSK provides satisfactory bit error rate (BER) for reliable transmission [1]. However, its transmission efficiency is low due to the requirement of transmitting two sequences in different time slots for one symbol, while highly complex delay line circuits are also involved.

To enhance efficiency, M-ary modulation schemes using Hilbert transform [8], [9], Walsh code [10], and index modulation [11] have been proposed, but they do not address the delay line issue. Instead, delay lines can be avoided by arranging different sequences in different subcarriers rather than in different time slots, which is the key idea behind multi-carrier (MC) transmission. Since one reference sequence can be used for demodulating multiple information-bearing sequences, MC-based DCSK systems can achieve significantly higher efficiency than the conventional counterparts [12]. To further reduce the computational complexity of MC-DCSK, the orthogonal frequency division multiplexing (OFDM) has been applied with the use of fast Fourier transform (FFT) [13]. Comparing with OFDM spread spectrum, OFDM-DCSK has enhanced security with smaller number of subcarriers [14].

However, the sensitivity of OFDM to Doppler shift, or time selective fading, is a significant concern. The Doppler effect, caused by the relative motion between the transmitter and receiver, can notably degrade performance in high-mobility scenarios [15] like V2V communication [16]. Indeed, Doppler shift can lead to inter-carrier interference (ICI) [17], which impairs the performance of OFDM-based DCSK systems. Various adaptations of OFDM-DCSK have been developed to combat these issues. For instance, [18] proposed a frequency-

Manuscript received 11 December, 2023. (*Corresponding author: Lin Zhang.*)

Zhaofeng Liu, Hing Cheung So and Zhi-Yong Wang are with Department of Electrical Engineering, City University of Hong Kong, Hong Kong SAR, China (e-mail: zhaofeliu3-c@my.cityu.edu.hk; hcso@ee.cityu.edu.hk; z.y.wang@my.cityu.edu.hk).

Lin Zhang is with School of Cyber Science and Technology, Sun Yat-sen University, Shenzhen, China (e-mail: isszl@mail.sysu.edu.cn).

Xiao Peng Li is with the College of Electronics and Information Engineering, Shenzhen University, Shenzhen, China (e-mail: x.p.li.frank@gmail.com).

hopping-based method to mitigate multipath fading. However, this approach does not consider Doppler shift. In another attempt, a pre-coding OFDM-DCSK system [19] was suggested to counteract the carrier frequency offset caused by Doppler shift. Despite its effectiveness, this method duplicates information symbols, thus compromising efficiency. In addition to the time selective fading due to high mobility, multi-path propagation caused by reflections from surrounding buildings and objects can induce rapid variations in the channel characteristics across different frequencies. This is referred to as doubly selective fading where the channel experiences significant variations over both time and frequency. As a matter of fact, high mobility communication scenarios are particularly susceptible to doubly selective fading. To tackle these fading channels, [20] designed a Walsh-coded OFDM-DCSK system. However, its complexity is high due to the long vector input to the FFT module. Therefore, further research and development are needed to enhance the performance of OFDM-based DCSK systems in high-mobility scenarios.

In this paper, we exploit singular value decomposition (SVD) to improve OFDM-DCSK system reliability over doubly selective fading channels. The primary motivation and novelty of this paper lie in achieving smaller BERs over doubly selective fading channels through SVD-based pre-coding. When channel state information (CSI) is available, SVD can decompose the channel into independent sub-channels. This is achieved by multiplying the symbol matrix at the transmitter with the right singular vectors. Moreover, by means of the water-filling principle, the symbols are strategically redistributed to achieve lower BER. The proposed channel decomposition and symbol reallocation can increase the signal-to-noise ratio (SNR) under doubly selective fading, thereby significantly improving the system reliability.

Our novelty and technical contributions are:

(i) We propose the singular-vector pre-coded OFDM-DCSK (SVP-OFDM-DCSK) system for reliability improvement over doubly selective fading channels.

(ii) The BER of the SVP-OFDM-DCSK system is analyzed. Additionally, we provide a rationale for assigning the largest singular value to the reference sequence in case when symbol reassignment is not performed.

(iii) We demonstrate that our approach attains lower BERs than existing systems [13], [18], [20], [21] over doubly selective fading channels.

We use bold upper-case and lower-case letters to represent matrices and vectors, respectively. The superscripts $(\cdot)^T$ and $(\cdot)^H$ denote transpose and Hermitian transpose, respectively. $\mathrm{vec}(\cdot)$ denotes the vectorization in column-major order, and $\mathrm{vec}^{-1}(\cdot)$ is the reverse process. In addition, $\mathbb{E}\{\cdot\}$ denotes the expectation operator, and $\mathrm{var}\{\cdot\}$ calculates the variance. Moreover, $\mathrm{diag}(\cdot)$ converts a vector to a diagonal matrix. Besides, $\Re\{\cdot\}$ stands for the real part of a complex-valued number or vector. Finally, $\mathbb{R}$ and $\mathbb{C}$ denote the sets of real and complex numbers, respectively.

II. SVP-OFDM-DCSK System

In this section, we present the structure of SVP-OFDM-DCSK system.

A. Transmitter Design

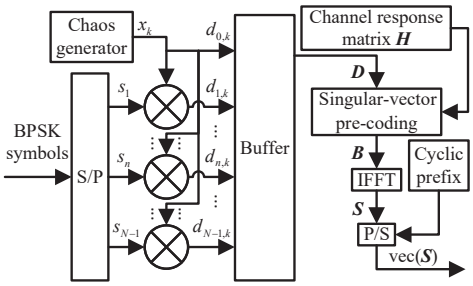

Fig. 1. Block diagram of SVP-OFDM-DCSK transmitter.

Figure 1 depicts the block diagram of the proposed transmitter. The main modification compared to the conventional OFDM-DCSK [13] is the introduction of singular-vector pre-coding prior to performing inverse FFT (IFFT). The chaos generator initially produces chaotic sequences using the second-order Chebyshev polynomial function, which is $x_{k+1} = 1 - 2x_k^2$, where $x_k \in (-1, 0) \cup (0, 1)$. Here, x_k denotes the kth chaotic chip, where $0 \leq k \leq \beta - 1$ with β being the sequence length. Chaotic modulation is then executed by multiplying the sequence with the BPSK data symbols carrying information bits after the serial-to-parallel (S/P) conversion. The kth chip associated with the nth subcarrier, corresponds to the (n, k) element of $\boldsymbol{D} = [\boldsymbol{d}_0\ \boldsymbol{D}_{N-1}]^T$, represented as $d_{n,k} = s_n x_k$. In this context, $\boldsymbol{d}_0 = [d_{0,0}, \cdots, d_{0,\beta-1}]^T$ acts as the reference sequence, while $\boldsymbol{D}_{N-1}$ signifies all $N-1$ sequences bearing information. Indices ranging from $1 \leq n \leq N-1$ are associated with sequences that carry information, while $n = 0$ is tied to the reference sequence defined by $d_{0,k} = x_k$.

Following chaotic modulation, the system conducts singular-vector pre-coding. During this phase, a permutation matrix $\boldsymbol{P}$ is adopted to rearrange the symbol matrix and the receiver is aware of $\boldsymbol{P}$. The goal of this operation is to reassign symbols with larger magnitudes to sub-channels that exhibit bigger gains. Adopting the water-filling principle, the symbol reassignment results in an increased SNR and hence improved BER performance. The implementation of permutation matrix is intended to replicate this advantageous distribution. Moreover, in correlation demodulation of DCSK, the correlation value is computed by multiplying symbols of matching indices from two sequences and summing these products. Given the variable magnitudes of symbols within a sequence, if larger symbols in chaotic sequences benefit from greater channel gains, the auto-correlation value could markedly increase, facilitating more effective demodulation and reduced BER. The permutation matrix $\boldsymbol{P}$ is employed to fulfill this purpose. With permutation, all large-magnitude symbols across sequences are allocated to sub-channels with higher gains, resulting in elevated correlation value and lower BER. Consequently, the BER performance with permutation can be superior to that without permutation, especially at low SNR. The matrix $\boldsymbol{P}$ has the form of:

$$\boldsymbol{P} = \begin{bmatrix} \boldsymbol{I}_\beta & \boldsymbol{0}; \ \boldsymbol{0} & \tilde{\boldsymbol{P}} \end{bmatrix} \tag{1}$$

where the $\beta \times \beta$ identity matrix $\boldsymbol{I}_\beta$ indicates that the reference sequence is not permuted, and the sub-channel associated with

the largest singular value is assigned to the reference. To determine $\tilde{\boldsymbol{P}}$, we first denote the vector prior to permutation as $\boldsymbol{d} = \text{vec}(\boldsymbol{D}_{N-1}) = [d_0, \cdots, d_{(N-1)\beta-1}]^T \in \mathbb{R}^{(N-1)\beta}$. Subsequent to the permutation, the vector is arranged in descending order of magnitude. We define the sorted vector as $\tilde{\boldsymbol{d}} = [\tilde{d}_0, \cdots, \tilde{d}_{(N-1)\beta-1}]^T \in \mathbb{R}^{(N-1)\beta}$, The use of $\tilde{\boldsymbol{P}}$ is to transform $\boldsymbol{d}$ into the sorted vector $\tilde{\boldsymbol{d}}$, which can be expressed as $\tilde{\boldsymbol{d}} = \tilde{\boldsymbol{P}}\boldsymbol{d}$. Mathematically, the permutation process is written as:

$$\tilde{\boldsymbol{D}} = (\text{vec}^{-1}(\boldsymbol{P}\text{vec}(\boldsymbol{D}^T)))^T \in \mathbb{R}^{N\times\beta}. \tag{2}$$

This method of sequence and symbol allocation in our system, while distinct in its mechanics, is similar in idea to the water-filling principle. $\boldsymbol{P}$ is sent from the transmitter to the receiver via specific control channel [19] and the synchronization of $\boldsymbol{P}$ is assumed perfect. If the transmitter and receiver cannot share $\boldsymbol{P}$, then the permutation step will not be performed, then we have $\boldsymbol{P} = \boldsymbol{I}$ and $\tilde{\boldsymbol{D}} = \boldsymbol{D}$.

After the permutation step, symbols are pre-coded using the singular vectors. The pre-coding is based on CSI, while obtaining CSI requires pilot-based channel estimation and increases the complexity from $\mathcal{O}(N\beta\log_2 N)$ to $\mathcal{O}(N^2\beta)$. This method gathers channel information at both transmitter and receiver by comparing received and original pilot signals to identify signal alterations. The CSI is then feedback to the transmitter, allowing access to it. When the channel response matrix $\boldsymbol{H}$ is known, SVD can be utilized, such that

$$\boldsymbol{F}\boldsymbol{H}\boldsymbol{F}^H/N = \boldsymbol{U}\boldsymbol{\Sigma}\boldsymbol{V}^H \tag{3}$$

where $\boldsymbol{F}$ is the FFT matrix while $\boldsymbol{U}$ and $\boldsymbol{V}$ are orthonormal matrices. In this case, the diagonal elements of $\boldsymbol{\Sigma}$ represent the singular values of $\boldsymbol{H}$, which are arranged in a descending order. The pre-coding process entails multiplying $\boldsymbol{V}$ with $\tilde{\boldsymbol{D}}$ to decompose the channel, which is represented as:

$$\boldsymbol{B} = \boldsymbol{V}\tilde{\boldsymbol{D}}. \tag{4}$$

Subsequently, IFFT is performed on $\boldsymbol{B}$, denoted as $\boldsymbol{S} = \boldsymbol{F}^H\boldsymbol{B}/\sqrt{N}$. At the end of the transmitter, the parallel data streams, which are contained in distinct rows of $\boldsymbol{S}$, are converted into a serial format via the parallel-to-serial (P/S) converter, corresponding to the operator $\text{vec}(\boldsymbol{S})$.

B. Receiver Design

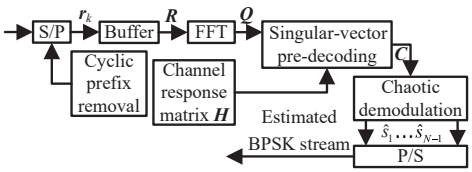

Fig. 2. Block diagram of SVP-OFDM-DCSK receiver.

The structure of the receiver is depicted in Fig. 2. The process begins with the received data undergoing cyclic prefix (CP) removal and S/P conversion. The received symbols are then assembled to form the matrix $\boldsymbol{R}$, which has the form of:

$$\boldsymbol{R} = [\boldsymbol{r}_0, \cdots, \boldsymbol{r}_k, \cdots, \boldsymbol{r}_{\beta-1}] = \boldsymbol{H}\boldsymbol{S} + \boldsymbol{N} \tag{5}$$

where $\boldsymbol{r}_k$ is the kth column of $\boldsymbol{R}$ and $\boldsymbol{N}$ is the Gaussian noise matrix. For doubly selective fading channels, $\boldsymbol{H}$ is written as $\boldsymbol{H} = \sum_{m=1}^{M} h_m \boldsymbol{T}_{\tau_m}\boldsymbol{\Delta}_{f_m}$, where M is the number of paths and h_m is a complex Gaussian distributed fading factor, while τ_m is the delay and f_m is a factor by which the Doppler shift of the mth path exceeds the bandwidth of a subcarrier, respectively. When $f_m > 1$, the Doppler shift surpasses the bandwidth of the subcarrier. Furthermore, $\boldsymbol{T}_{\tau_m}$ and $\boldsymbol{\Delta}_{f_m}$ are expressed as [22]:

$$\boldsymbol{T}_{\tau_m} = \begin{bmatrix}\boldsymbol{0} & \boldsymbol{I}_{\tau_m}; & \boldsymbol{I}_{N-\tau_m} & \boldsymbol{0}\end{bmatrix} \tag{6}$$

$$\boldsymbol{\Delta}_{f_m} = \text{diag}\left(\left[e^{\frac{j2\pi f_m\cdot 0}{N}}, e^{\frac{j2\pi f_m\cdot 1}{N}}, \cdots, e^{\frac{j2\pi f_m\cdot(N-1)}{N}}\right]\right) \tag{7}$$

where $\boldsymbol{0}$ denotes the zero matrix. We assume that for doubly selective fading, the symbol duration is larger than the coherence time or the reciprocal of maximum Doppler shift, and the bandwidth of transmitted signal is larger than the coherence bandwidth or the reciprocal of maximum delay.

Next, FFT is applied to $\boldsymbol{R}$, resulting in $\boldsymbol{Q}$, which is expressed as $\boldsymbol{Q} = \boldsymbol{F}\boldsymbol{R}/\sqrt{N}$. Utilizing the left singular vector matrix $\boldsymbol{U}$, the initial step of singular-vector pre-decoding involves multiplying $\boldsymbol{U}^H$ by $\boldsymbol{Q}$. In accordance with (3)-(5), we deduce:

$$\begin{aligned}\tilde{\boldsymbol{C}} &= \boldsymbol{U}^H\boldsymbol{Q} = \boldsymbol{U}^H\boldsymbol{F}\boldsymbol{R}/\sqrt{N} = \boldsymbol{U}^H\boldsymbol{F}(\boldsymbol{H}\boldsymbol{S}+\boldsymbol{N})/\sqrt{N}\\ &= \boldsymbol{U}^H\boldsymbol{F}\boldsymbol{H}\boldsymbol{F}^H\boldsymbol{B}/N + \boldsymbol{U}^H\boldsymbol{F}\boldsymbol{N}/\sqrt{N}\\ &= \boldsymbol{U}^H\boldsymbol{F}\boldsymbol{H}\boldsymbol{F}^H\boldsymbol{V}\tilde{\boldsymbol{D}}/N + \boldsymbol{U}^H\boldsymbol{F}\boldsymbol{N}/\sqrt{N}\\ &= \boldsymbol{\Sigma}\tilde{\boldsymbol{D}} + \boldsymbol{U}^H\boldsymbol{F}\boldsymbol{N}/\sqrt{N}.\end{aligned} \tag{8}$$

As inferred from (8), the useful signal component in $\tilde{\boldsymbol{C}}$ is $\boldsymbol{\Sigma}\tilde{\boldsymbol{D}}$. Since $\boldsymbol{\Sigma}$ is a positive diagonal matrix, $\tilde{\boldsymbol{C}}$ can be seen as a scaled variant of $\tilde{\boldsymbol{D}}$, where each row signifies a sub-channel with a unique channel gain. This implies that all symbols in $\tilde{\boldsymbol{D}}$ are positively scaled without any phase change, which is advantageous for the subsequent correlation-based BPSK demodulation. For conventional systems without pre-coding, the BER performance degrades severely due to the phase of complex fading coefficients and inter-carrier interference (ICI). The proposed scheme effectively converts the non-diagonal channel frequency response matrix $\boldsymbol{F}\boldsymbol{H}$ into a product of a non-negative diagonal matrix and the desired signal, thus alleviating the detrimental effects of ICI and outperforming the conventional systems over doubly selective fading channels. The subsequent step in singular-vector pre-decoding involves recovering the symbol matrix from the permuted matrix. This process is mathematically written as:

$$\boldsymbol{C} = \Re\{\text{vec}^{-1}(\boldsymbol{P}^T\text{vec}(\tilde{\boldsymbol{C}}^T))\} \in \mathbb{R}^{\beta\times N}. \tag{9}$$

Note that the permutation matrix has the property of $\boldsymbol{P}^T = \boldsymbol{P}^{-1}$. Each column vector of $\boldsymbol{C}$ represents a chaotic sequence, with the first one $\boldsymbol{c}_0$ serving as the reference sequence, and the remaining being information-bearing sequences. The detected BPSK symbol $\hat{s}_n$ is obtained through chaotic demodulation as

$$\hat{s}_n = \text{sgn}(Z_n) = \text{sgn}\left(\boldsymbol{c}_0^T\cdot\boldsymbol{c}_n\right), \quad 1 \le n \le N-1 \tag{10}$$

where $\text{sgn}(\cdot)$ denotes the sign function, $Z_n = \boldsymbol{c}_0^T\cdot\boldsymbol{c}_n$, and $\boldsymbol{c}_n$ represents the sequence for the nth symbol. Lastly, the information bits are directly decoded from the BPSK symbols.

III. BER Analysis

In the BER analysis, it is assumed that the fading parameters remain unchanged during the duration of the SVP-OFDM-DCSK symbol. Additionally, we presume that β is sufficiently large, thereby enabling us to apply the Gaussian approximation (GA) method [23], [24] to derive the BER expression. In (8), the term $\boldsymbol{U}^H\boldsymbol{F}\boldsymbol{N}/\sqrt{N}$ also represents Gaussian noise, as the Gaussian random variable remains Gaussian after being orthogonally transformed. Consequently, the post-permutation symbol can be expressed as $c_{n,k} = \sigma_{n,k}d_{n,k} + \xi_{n,k}$, where $\sigma_{n,k}$ is a singular value in $\boldsymbol{\Sigma}$ and $\xi_{n,k}$ follows a zero-mean Gaussian distribution with power $N_0/2$. Notably, when $n = 0$, the singular value corresponding to the reference sequence is $\sigma_{0,k} = \sigma_*$, where σ_* represents the largest singular value. Due to permutation, $\sigma_{n,k}$ for $n \geq 1$ is determined by $d_{n,k}$, and $\sigma_{n,k}$ for $n = 0$ is the largest singular value. Following this, from (10), we have [18]:

$$\begin{aligned} Z_n &= \sum_{k=0}^{\beta-1} c_{0,k}c_{n,k} = \sum_{k=0}^{\beta-1} (\sigma_* d_{0,k} + \xi_{0,k})(\sigma_{n,k}d_{n,k} + \xi_{n,k}) \\ &= P_1 + P_2 + P_3 \end{aligned} \tag{11}$$

where $P_1 = \sum_{k=0}^{\beta-1} s_n\sigma_*\sigma_{n,k}x_k^2$ represents the desired signal, while $P_2 = \sum_{k=0}^{\beta-1} \xi_{0,k}\xi_{n,k}$ and $P_3 = \sum_{k=0}^{\beta-1}(\sigma_* x_k\xi_{n,k} + s_n\sigma_{n,k}x_k\xi_{0,k})$ denote disturbance components. As P_1, P_2, and P_3 are statistically independent, the expected value and variance of Z_n can be calculated as [18]:

$$\begin{aligned} \mathbb{E}\{Z_n|(s_n = \pm 1)\} &= \sum_{l=1}^{3} \mathbb{E}\{P_l|(s_n = \pm 1)\} \\ \mathrm{var}\{Z_n|(s_n = \pm 1)\} &= \sum_{l=1}^{3} \mathrm{var}\{P_l|(s_n = \pm 1)\}. \end{aligned} \tag{12}$$

Proceeding further, we use the central limit theorem to uncover the statistical characteristics of P_1, P_2, and P_3 as follows:

$$\mathbb{E}\{P_1|s_n = +1\} = -\mathbb{E}\{P_1|s_n = -1\} = \beta\sigma_*\mathbb{E}\{\sigma_{n,k}x_k^2\} \tag{13a}$$

$$\mathbb{E}\{P_2|s_n = \pm 1\} = \mathbb{E}\{P_3|s_n = \pm 1\} = 0 \tag{13b}$$

$$\mathrm{var}\{P_1|s_n = \pm 1\} = \beta\sigma_*^2\mathrm{var}\left\{\sigma_{n,k}x_k^2\right\} \tag{13c}$$

$$\mathrm{var}\{P_2|s_n = \pm 1\} = \beta N_0^2/4 \tag{13d}$$

$$\mathrm{var}\{P_3|s_n = \pm 1\} = \beta N_0(\sigma_*^2\mathbb{E}\{x_k^2\} + \mathrm{var}\{\sigma_{n,k}x_k\})/2. \tag{13e}$$

The signal-to-interference-plus-noise ratio (SINR) is then defined as $\Gamma = \mathbb{E}\{Z_n|(s_n = \pm 1)\}^2/\mathrm{var}\{Z_n|(s_n = \pm 1)\}$. Over doubly selective fading channel, the BER of Z_n is [18]:

$$\begin{aligned} \mathrm{BER}_{Z_n}(\boldsymbol{\Sigma}) &= \mathrm{erfc}\left(\sqrt{\Gamma/2}\right)/2 \\ &= \mathrm{erfc}\left[\left(2\mathrm{var}\{Z_n|(s_n = \pm 1)\}/\mathbb{E}\{Z_n|(s_n = \pm 1)\}^2\right)^{-\frac{1}{2}}\right]/2 \end{aligned} \tag{14}$$

where $\mathrm{var}\{Z_n|(s_n = \pm 1)\}$ and $\mathbb{E}\{Z_n|(s_n = \pm 1)\}^2$ are calculated based on (12) and (13). The function $\mathrm{erfc}(\cdot)$ is the complementary error function.

When no permutation is implemented, each chaotic sequence possesses a unique singular value, symbolized as $\sigma_{n,k} = \sigma_n$. Consequently, we have $\mathbb{E}\{\sigma_{n,k}x_k^2\} = \sigma_n\mathbb{E}\{x_k^2\}$, $\mathrm{var}\left\{\sigma_{n,k}x_k^2\right\} = \sigma_n^2\mathrm{var}\left\{x_k^2\right\}$ and $\mathrm{var}\{\sigma_{n,k}x_k\} = \sigma_n^2\mathbb{E}\{x_k^2\}$, where the mean and variance of x_k^2 are $\mathbb{E}\{x_k^2\} = 1/2$ and $\mathrm{var}\{x_k^2\} = 1/8$, respectively. Defining $E_b = N\beta\mathbb{E}\{x_k^2\}/(N-1)$ as the energy consumption per bit, when no permutation is applied, the term enclosed within (14) is given as:

$$\begin{aligned} \left(\frac{2\mathrm{var}\{Z_n|(s_n = \pm 1)\}}{\mathbb{E}\{Z_n|(s_n = \pm 1)\}^2}\right)_{\mathrm{np}} &= \frac{\frac{1}{2}N^2\beta}{(N-1)^2\sigma_*^2\sigma_n^2}\left(\frac{N_0}{E_b}\right)^2 \\ &+ \frac{(\sigma_*^2 + \sigma_n^2)N}{\sigma_*^2\sigma_n^2(N-1)}\frac{N_0}{E_b} + \frac{1}{\beta}. \end{aligned} \tag{15}$$

In cases where the singular value assigned to the reference sequence is less than σ_*, (15) yields a greater value. This subsequently leads to a higher BER as stipulated in (14). Therefore, assigning the largest singular value to the reference results in lower BER. Considering that the singular values are randomly distributed in response to channel fading, BER_{Z_n} is consequently a function of $\boldsymbol{\Sigma}$. Therefore, to compute the final BER, we take the expected value of BER_{Z_n} across all admissible $\boldsymbol{\Sigma}$ as $\mathrm{BER}_{\mathrm{all}} = \mathbb{E}_n\left\{\int \mathrm{BER}_{Z_n}(\boldsymbol{\Sigma})p(\boldsymbol{\Sigma})d\boldsymbol{\Sigma}\right\}$, where $p(\boldsymbol{\Sigma})$ is the probability density function of $\boldsymbol{\Sigma}$ which is numerically determined, while $\mathbb{E}_n\{\cdot\}$ signifies the expectation taken over Z_n across all values of n.

IV. Simulation Results

We have conducted simulations to evaluate the performance of the SVP-OFDM-DCSK system. The total number of subcarriers is $N = 64$, while the chaotic sequence length is $\beta = 50$.

The BER performance of the proposed system is contrasted with existing systems including the frequency hoping (FH) OFDM-DCSK [18], frequency domain equalization (FDE) OFDM-DCSK [13], [21], and OFDM code shifted (CS) DCSK [20]. The E_b/N_0 range is set as $[0, 50]$ dB. For each E_b/N_0, simulations are performed on more than 500000 bits. To demonstrate the results over doubly fading channels, we establish two distinct channel configurations. The first configuration consists of 4 paths, each possessing an average power of $1/4$, and the second configuration includes 8 paths, each with an average power of $1/8$. The delay and the Doppler shift are defined as in (6) and (7), and are set as $\tau_m = f_m = m - 1$ where integer m spans a range from 1 to 4 for the case with 4 paths, and varies from 1 to 8 in the 8-path scenario. Furthermore, it is assumed that perfect CSI is obtained for FDE-OFDM-DCSK [13], [21] at the receiver.

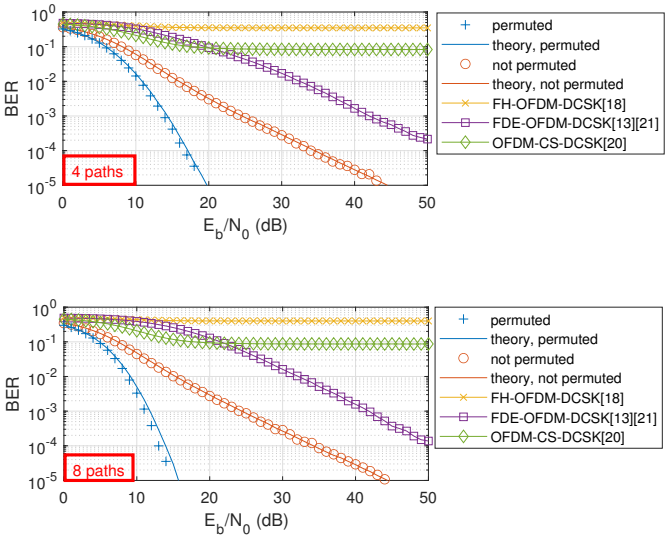

Fig. 3. BER versus E_b/N_0.

Figure 3 plots the BER over the doubly selective fading channel against E_b/N_0 for the proposed system, as well as FH-OFDM-DCSK [18], FDE-OFDM-DCSK [13], [21], and OFDM-CS-DCSK [20]. When permutation is performed, the transceiver is required to share permutation parameters, which may pose implementation challenges. Consequently, we exhibit the results of our system both with and without permutation. The theoretical BERs are also included. A notable observation is the close agreement between the theoretical and simulated BERs. Moreover, the BER undergoes a significant decrease when the permutation step is integrated. When the path number increases from 4 to 8, there is a decrease in the BER for the permuted configuration. This decline can be attributed to the acquisition of diversity gain.

Comparing the proposed system with the competitors, it is clear that those designed for frequency selective fading channels, namely, FH-OFDM-DCSK [18] and FDE-OFDM-DCSK [13], [21], yield higher BER. Additionally, we have included OFDM-CS-DCSK [20] for comparison as it is specifically designed for doubly selective fading channels. However, when the proposed system and OFDM-CS-DCSK operate with the same transmission efficiency, the latter performance is subpar, even revealing an error floor. This is attributed to the interference caused by the superimposition of the Walsh sequences in OFDM-CS-DCSK, which exacerbates as the sequence number increases. Conversely, the proposed system refrains from using the Walsh sequences and instead applies SVD to decompose the channel, thereby suffering less interference than OFDM-CS-DCSK. This strategy facilitates better BER performance over doubly selective fading channels.

V. Conclusion

An SVP-OFDM-DCSK system is devised by utilizing SVD for reliability improvement over doubly selective fading channels. In circumstances where CSI is accessible, the use of SVD has proven effective in decomposing the channel into distinct sub-channels, accomplished by employing right singular vectors in the multiplication of the symbol matrix at the transmitter. Subsequently, the sub-channel associated with the largest singular value is allocated to transmit the reference chaotic sequence, thereby enhancing the SNR at the receiver. Furthermore, we have demonstrated that symbol permutation according to the water-filling principle results in further SNR increase. This combined approach of channel decomposition and symbol reallocation boosts the SNR over the doubly selective channel, thereby significantly decreasing the BER and improving system reliability. The BER of the proposed system over doubly selective fading channel is also derived. Simulation results verify the BER derivation, and demonstrate that the proposed solution can attain lower BER than existing OFDM-DCSK systems.

References

[1] Y. Fang, G. Han, P. Chen, F. C. M. Lau, G. Chen, and L. Wang, "A survey on DCSK-based communication systems and their application to UWB scenarios," *IEEE Commun. Surv. Tutor.*, vol. 18, no. 3, pp. 1804–1837, July-Sept. 2016.

[2] F. C. M. Lau and C. K. Tse, *Chaos-Based Digital Communication Systems*. New York, NY, USA: Springer, 2003.

[3] H. Ma, G. Cai, Y. Fang, J. Wen, P. Chen, and S. Akhtar, "A new enhanced energy-detector-based FM-DCSK UWB system for tactile Internet," *IEEE Trans. Ind. Informat.*, vol. 15, no. 5, pp. 3028–3039, May 2019.

[4] G. Kaddoum and N. Tadayon, "Differential chaos shift keying: A robust modulation scheme for power-line communications," *IEEE Trans. Circuits Syst. II, Exp. Briefs*, vol. 64, no. 1, pp. 31–35, Jan. 2017.

[5] Z. Chen, L. Zhang, J. Zhang, Z. Wu, and D. Luobu, "An OFDM-based pre-coded chaos shift keying transceiver for reliable V2V transmission," *IEEE Trans. Veh. Technol.*, vol. 71, no. 6, pp. 6710–6715, June 2022.

[6] G. Kolumbán, B. Vizvári, W. Schwarz, and A. Abel, "Differential chaos shift keying: A robust coding for chaos communication," in *International Workshop on Nonlinear Dynamics of Electronic Systems*, Seville, Spain, June 1996, pp. 87–92.

[7] H. Cao, Y. T. Chan, and H. C. So, "Compressive TDOA estimation: Cramér-Rao bound and incoherent processing," *IEEE Trans. Aerosp. Electron. Syst.*, vol. 56, no. 4, pp. 3326–3331, Aug. 2020.

[8] Z. Galias and G. M. Maggio, "Quadrature chaos-shift keying: Theory and performance analysis," *IEEE Trans. Circuits Syst. I, Fundam. Theory Appl.*, vol. 48, no. 12, pp. 1510–1519, Dec. 2001.

[9] L. Wang, G. Cai, and G. R. Chen, "Design and performance analysis of a new multiresolution M-ary differential chaos shift keying communication system," *IEEE Trans. Wirel. Commun.*, vol. 14, no. 9, pp. 5197–5208, Sept. 2015.

[10] N. Li, J.-F. Martinez-Ortega, V. H. Díaz, and J. M. M. Chaus, "A new high-efficiency multilevel frequency-modulation different chaos shift keying communication system," *IEEE Syst. J.*, vol. 12, no. 4, pp. 3334–3345, Dec. 2018.

[11] Z. Liu, L. Zhang, Z. Wu, and Y. Jiang, "Energy efficient parallel concatenated index modulation and M-ary PSK aided OFDM-DCSK communications with QoS consideration," *IEEE Trans. Veh. Technol.*, vol. 69, no. 9, pp. 9469–9482, Sept. 2020.

[12] G. Kaddoum, F. D. Richardson, and F. Gagnon, "Design and analysis of a multi-carrier differential chaos shift keying communication system," *IEEE Trans. Commun.*, vol. 61, no. 8, pp. 3281–3291, Aug. 2013.

[13] S. Li, Y. Zhao, and Z. Wu, "Design and analysis of an OFDM-based differential chaos shift keying communication system," *J. Commun.*, vol. 10, no. 3, pp. 199–205, Mar. 2015.

[14] Q. Li, M. Wen, E. Basar, and F. Chen, "Index modulated OFDM spread spectrum," *IEEE Trans. Wirel. Commun.*, vol. 17, no. 4, pp. 2360–2374, 2018.

[15] Y. Li, N. Seshadri, and S. Ariyavisitakul, "Channel estimation for OFDM systems with transmitter diversity in mobile wireless channels," *IEEE J. Sel. Areas Commun.*, vol. 17, no. 3, pp. 461–471, 1999.

[16] Y. Fu, C.-X. Wang, Y. Yuan, R. Mesleh, e.-H. M. Aggoune, M. M. Alwakeel, and H. Haas, "BER performance of spatial modulation systems under 3-D V2V MIMO channel models," *IEEE Trans. Veh. Technol.*, vol. 65, no. 7, pp. 5725–5730, 2016.

[17] Y. Mostofi and D. Cox, "ICI mitigation for pilot-aided OFDM mobile systems," *IEEE Trans. Wirel. Commun.*, vol. 4, no. 2, pp. 765–774, 2005.

[18] Z. Liu, L. Zhang, Z. Wu, and J. Bian, "A secure and robust frequency and time diversity aided OFDM-DCSK modulation system not requiring channel state information," *IEEE Trans. Commun.*, vol. 68, no. 3, pp. 1684–1697, Mar. 2020.

[19] Z. Liu, L. Zhang, and Z. Wu, "Reliable and secure pre-coding OFDM-DCSK design for practical cognitive radio systems with the carrier frequency offset," *IEEE Trans. Cogn. Commun. Netw.*, vol. 6, no. 1, pp. 189–200, Mar. 2020.

[20] M. Chen, W. Xu, D. Wang, and L. Wang, "Design of a multi-carrier different chaos shift keying communication system in doubly selective fading channels," in *2017 23rd Asia-Pacific Conference on Communications (APCC)*, Dec. 2017, pp. 1–6.

[21] X. Ouyang and J. Zhao, "Single-tap equalization for fast OFDM signals under generic linear channels," *IEEE Commun. Lett.*, vol. 18, no. 8, pp. 1319–1322, Aug. 2014.

[22] P. Raviteja, Y. Hong, E. Viterbo, and E. Biglieri, "Practical pulse-shaping waveforms for reduced-cyclic-prefix OTFS," *IEEE Trans. Veh. Technol.*, vol. 68, no. 1, pp. 957–961, Jan. 2019.

[23] Y. Xia, C. K. Tse, and F. C. M. Lau, "Performance of differential chaos-shift-keying digital communication systems over a multipath fading channel with delay spread," *IEEE Trans. Circuits Syst. II, Exp. Briefs*, vol. 51, no. 12, pp. 680–684, Dec. 2004.

[24] M. Dawa, G. Kaddoum, and Z. Sattar, "A generalized lower bound on the bit error rate of DCSK systems over multi-path Rayleigh fading channels," *IEEE Trans. Circuits Syst. II, Exp. Briefs*, vol. 65, no. 3, pp. 321–325, Mar. 2018.